Electronic Supplementary Material (ESI) for Biomaterials Science.

Engineered human *H*-chain ferritin with reversed charge of internal cavity exhibits RNA-mediated sponge-like effect for loading of RNA/DNA binding molecules

Marketa Charousova[1,†], Marie Kudlickova Peskova[2,†], Paulina Takacsova[1], Katerina Kapolkova[1], Yazan Haddad[1], Jan Bilek[1], Ladislav Sivak[1], Tomas Bartejs[2], Zbynek Heger[1**], Vladimir Pekarik[1,2*]

[1]*Department of Chemistry and Biochemistry, Mendel University in Brno, Zemedelska 1, Brno CZ-613 00, Czechia*

[2]*Central European Institute of Technology, Masaryk University, Kamenice 5, Brno CZ-625 00, Czechia*

[†]*These authors contributed equally*

Corresponding Authors

*Vladimir Pekarik, Mendel University in Brno, Zemedelska 1, Brno CZ-613 00, Czechia; E-mail: vladimir.pekarik@mendelu.cz;

**Zbynek Heger, Mendel University in Brno, Zemedelska 1, Brno CZ-613 00, Czechia; E-mail: zbynek.heger@mendelu.cz; phone: +420-5-4513-3350.

Full-length protein sequences:

>**HsaFtH**

MTTASTSQVRQNYHQDSEAAINRQINLELYASYVYLSMSYYFDRDDVALKNFAKYF

LHQSHEEREHAEKLMKLQNQRGGRIFLQDIKKPDCDDWESGLNAMECALHLEKNVN

QSLLELHKLATDKNDPHLCDFIETHYLNEQVKAIKELGDHVTNLRKMGAPESGLAEY

LFDKHTLGD**SDNES**

>**HsaFtH-RK**

M**G**TTASTSQVRQNYHQDSEAAINRQINLELYASYVYLSMSYYFDRDDVALKNFAKY

FLHQSHEEREHAEKLMKLQNQRGGRIFLQDIKKPDCDDWESGLNAMECALHLEKNV

NQSLLELHKLATDKNDPHLCDFIETHYLNEQVKAIKELGDHVTNLRKMGAPESGLAE

YLFDKHTLG**RKRK**

Supplementary Figures:

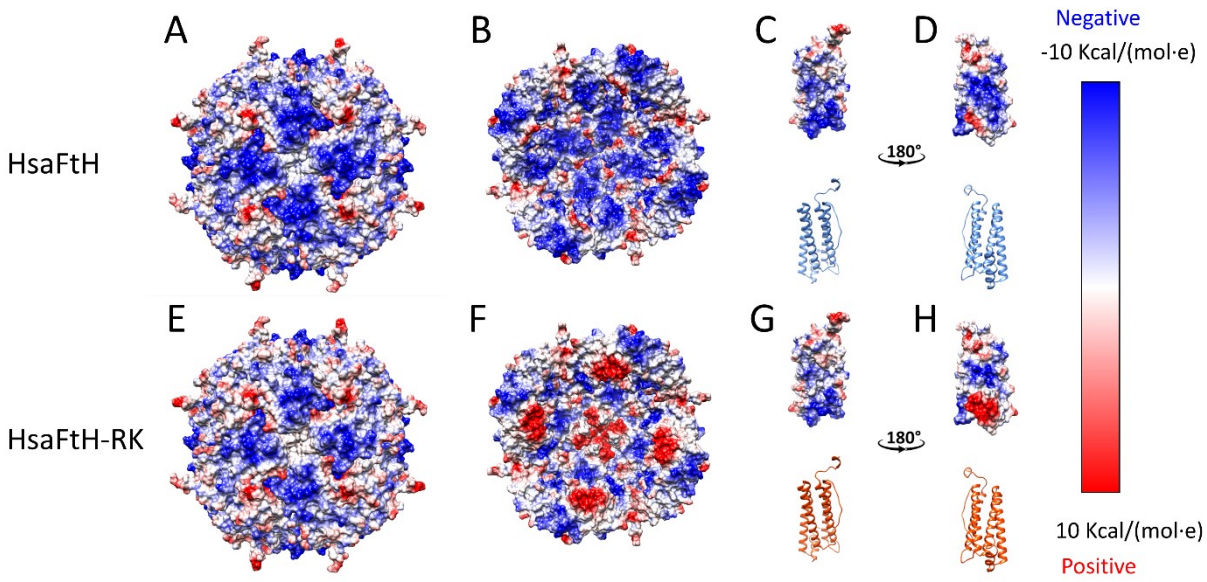

Fig. S1: Surface charge analysis of wild-type HsaFtH and HsaFtH-RK. Surface charge of the external surface of assembled ferritins (**A** and **E**) does not show any significant alteration. The internal surface of the HsaFtH-RK (**F**) shows an increase of positive charge in comparison to the wild-type HsaFtH (**B**). *In silico* models of individual subunits of wild-type (**C** and **D**) and HsaFtH-RK (**G** and **H**).

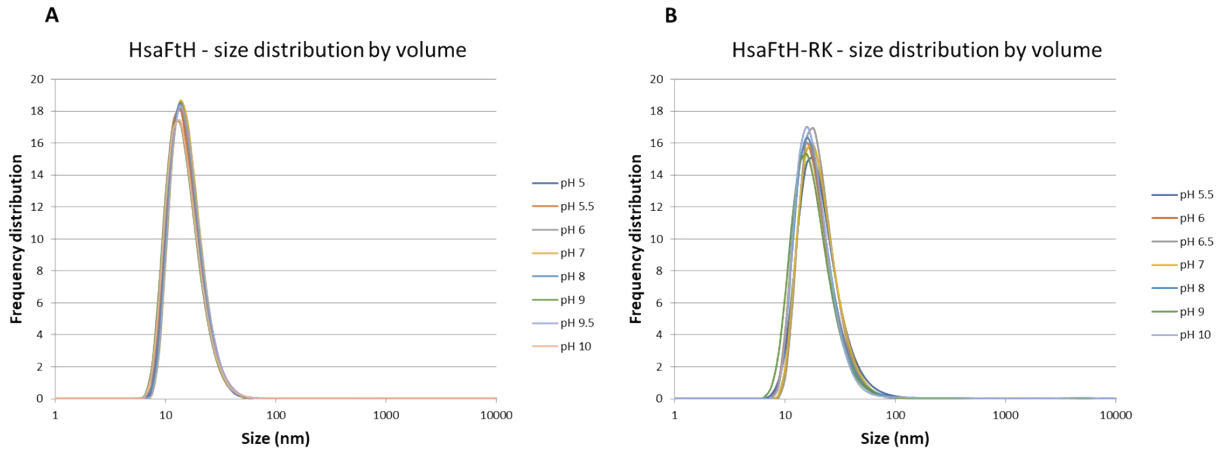

Fig. S2: Hydrodynamic diameter of HsaFTH and HsaFtH-RK analyzed by DLS. The results show that both proteins have homogenous size distribution in wide range of pH with (**A**) HsaFtH mean size of 13.5 nm, and (**B**) mean size of HsaFtH-RK of 15.7 nm.

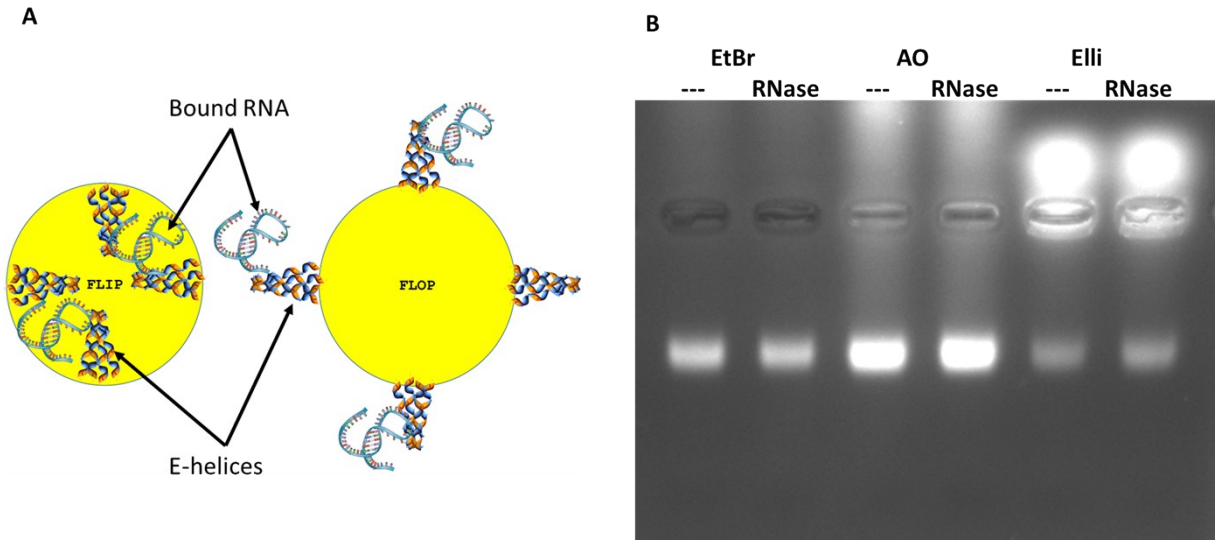

Fig. S3: (**A**) Presumptive orientation of E-helices in FLIP or FLOP manner with RNA bound to RKRK domain inside the HsaFtH-RK in FLIP orientation and outside in FLOP orientation. (**B**) HsaFtH-RK was treated with RNase A and then incubated with RNA binding dyes and separated on agarose gel. In case of acridine orange (AO) and ellipticine (Elli) clear staining of the gel above the wells due to migration of non-bound dye in opposite direction than HsaFtH-RK can be seen. No dye migrating in the direction of released RNA is observable. EtBr, ethidium bromide.

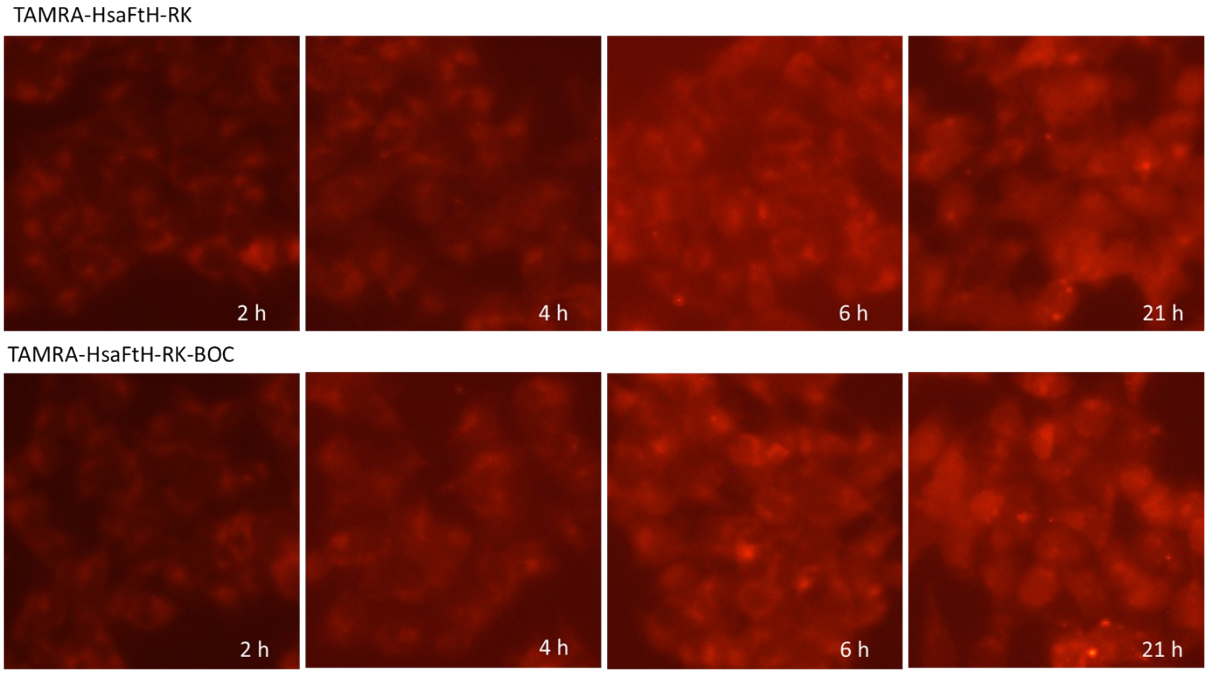

Fig. S4: The kinetics of cellular uptake of TAMRA-HsaFtH-RK and TAMRA-HsaFtH-RK-BOC. Scale bar, 20 μm.

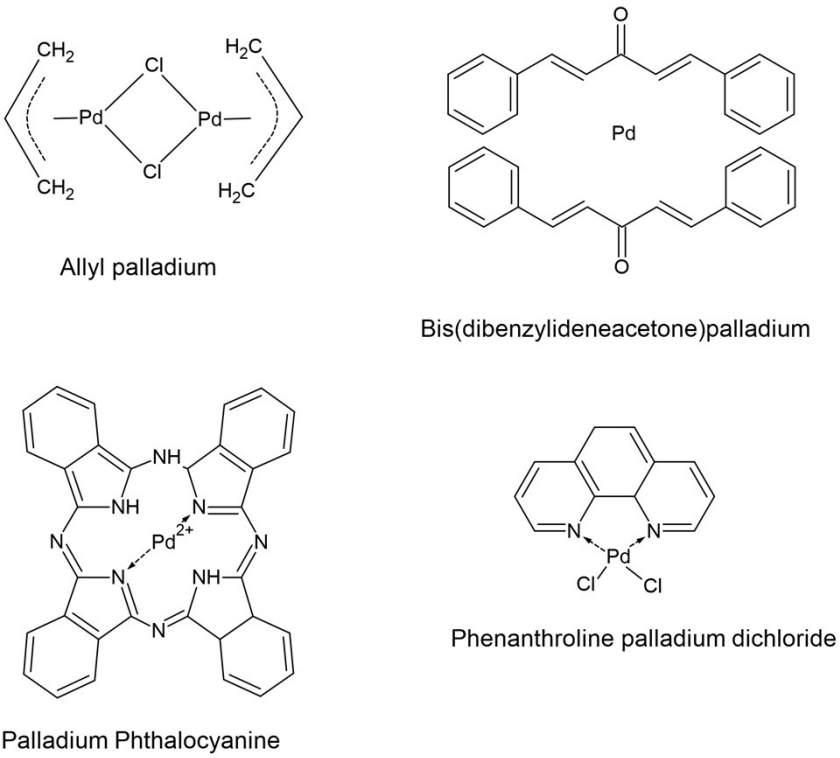

Fig. S5: Chemical formulas of tested palladium complexes

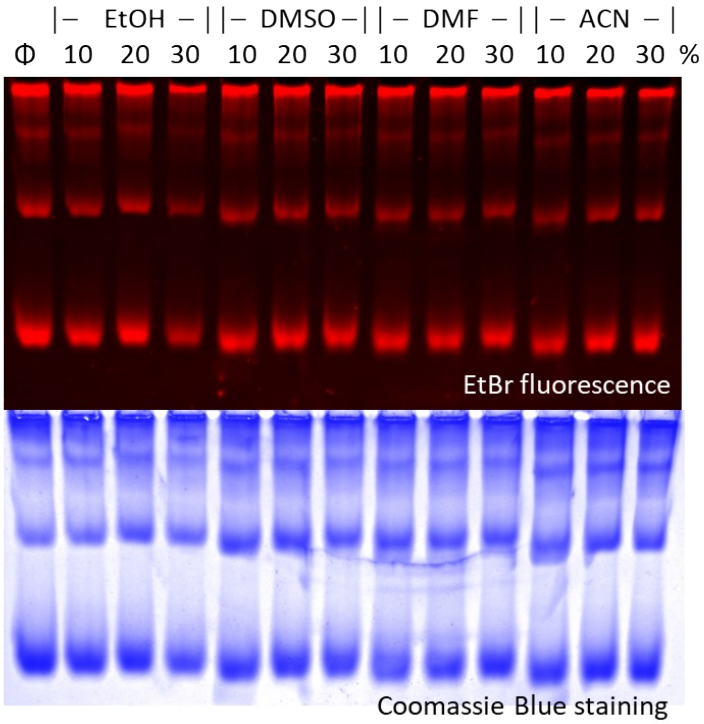

Fig. S6: Stability of HsaFtH-RK in presence of organic solvents. Even with concentrations up to 30% of the solvents, no protein aggregation and subsequent RNA shedding is present. EtOH, ethanol; DMSO, dimethylsulfoxide; DMF, dimethylformamide; ACN, acetonitrile.

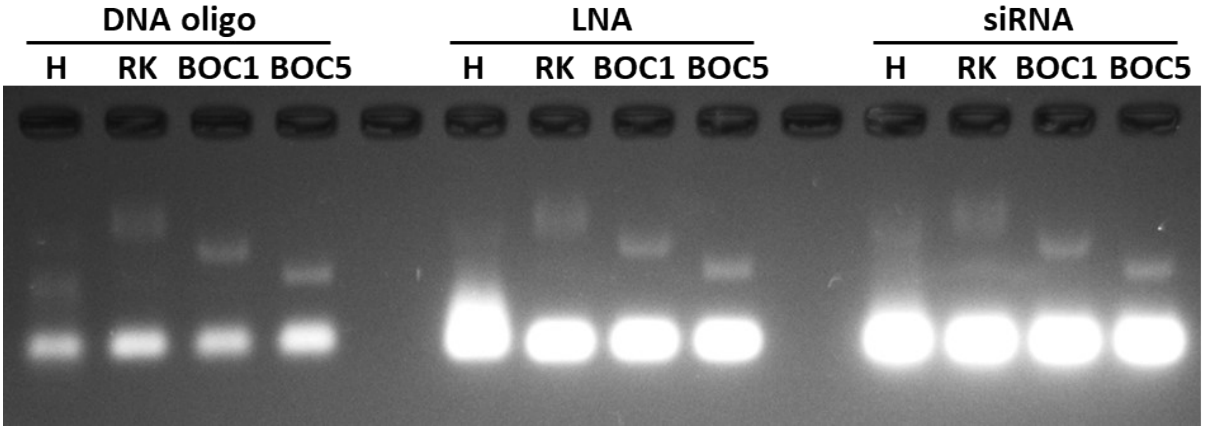

Figure S7: Loading of *wt* HsaFtH, HsaFtH-RK and BOC-HsaFtH-RK (1 or 5 mM) with Cy3-labelled DNA, FITC-labeled LNA and FAM-labelled siRNA. The gel shows the specific band of loaded HsaFtH-RK and its migration after surface modification with BOC. Either no band or smear highlighting no loading to *wt* HsaFtH can be seen.

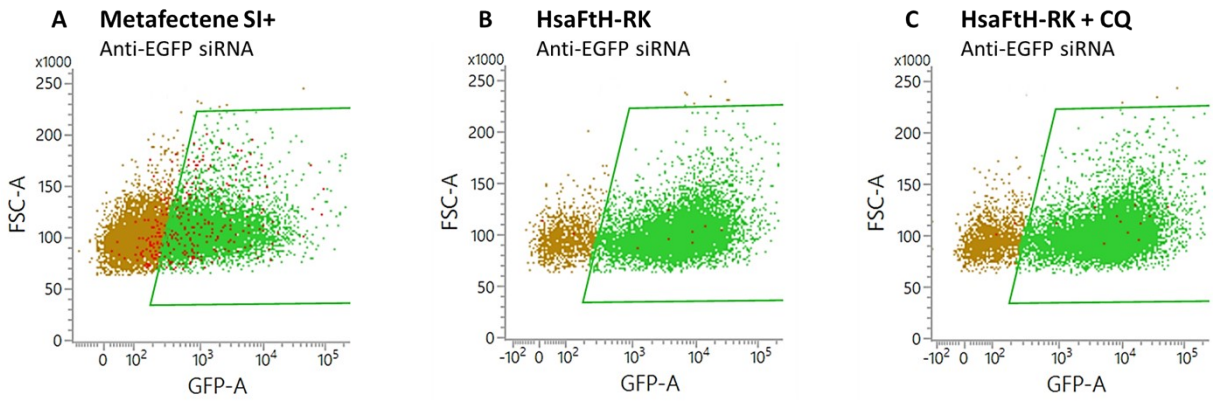

Fig. S8: FACS plots of RNA interference triggered by anti-EGFP siRNA in d2EGFP^{+} HEK-293 cells. (**A**) siRNA transfected with commercial transfection reagent Metafectene SI+, (**B**) siRNA transfected with HsaFtH-RK, and (**C**) siRNA transfected with HsaFtH-RK and treated with chloroquine (CQ). The cells were administered for 72 hours.

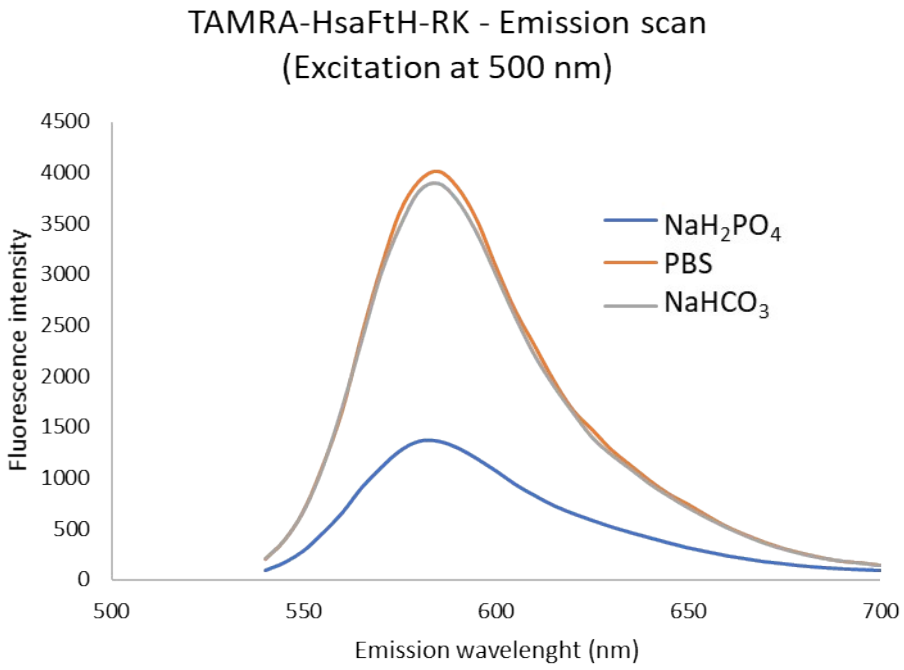

Fig. S9: pH-responsive fluorescence emission of TAMRA-HsaFtH-RK analyzed in 100 mM NaH_2PO_4 with pH 5.5, PBS with pH 7.4, and 100 mM $NaHCO_3$ with pH 8.5

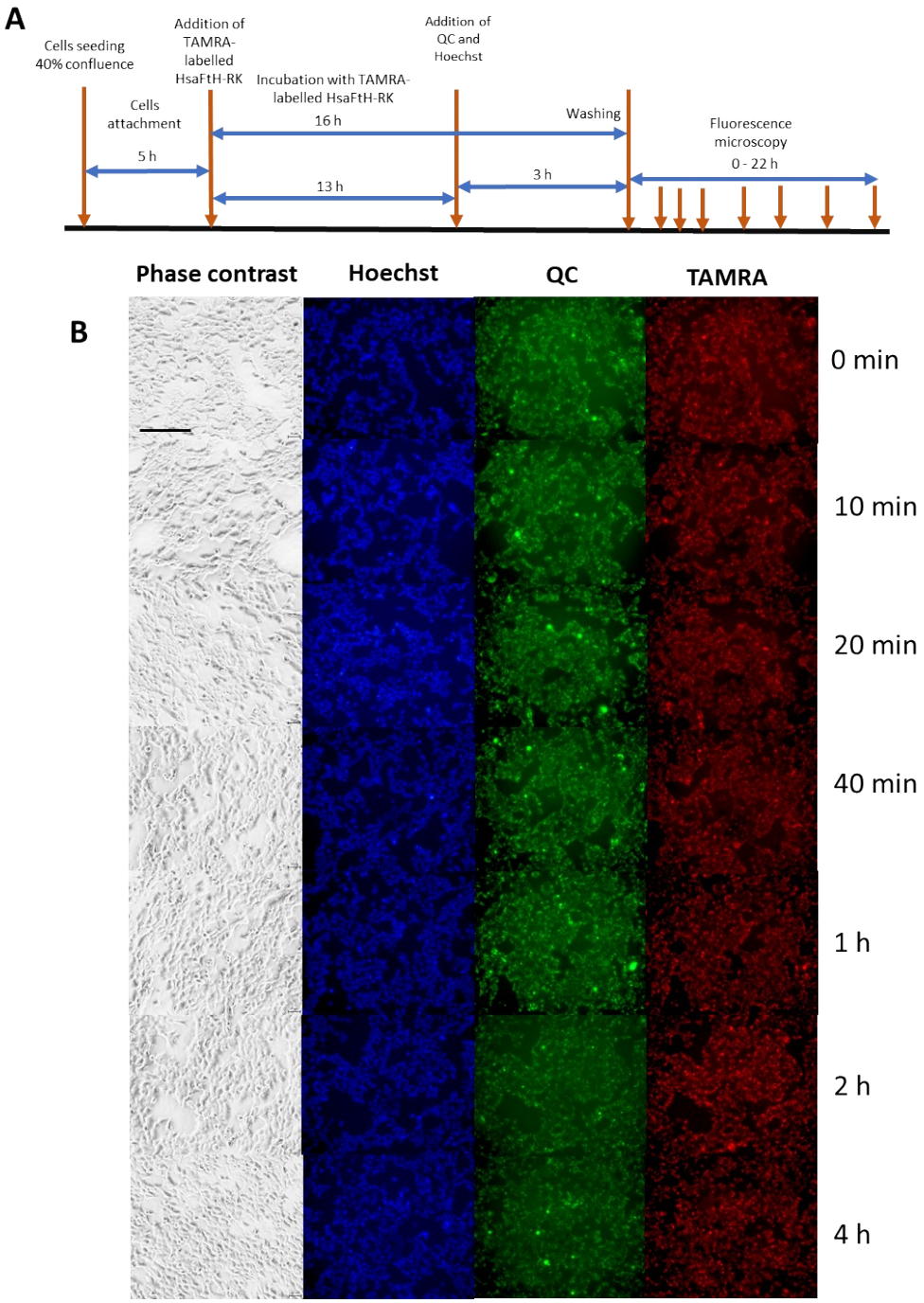

Fig. S10: HEK-293 cells treated with TAMRA-HsaFtH-RK. The acidic endolysosomal compartments are stained using QC. (**A**) Schematic drawing of experiment time-course and treatment regimes. (**B**) Phase contrast and fluorescence micrographs of TAMRA-HsaFtH-RK treated HEK-293 cells in indicated time points. Nuclei were counterstained using Hoechst 33342. Scale bar, 200 µm.

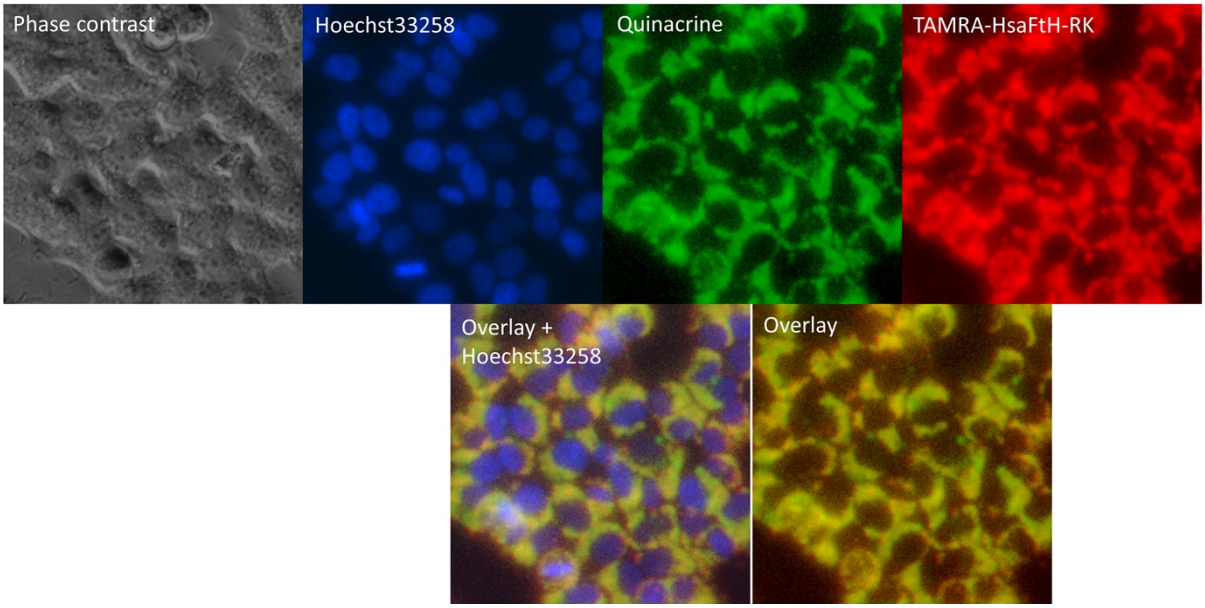

Fig S11: Colocalization of lysosomal marker quinacrine with TAMRA labelled HsaFtH-RK

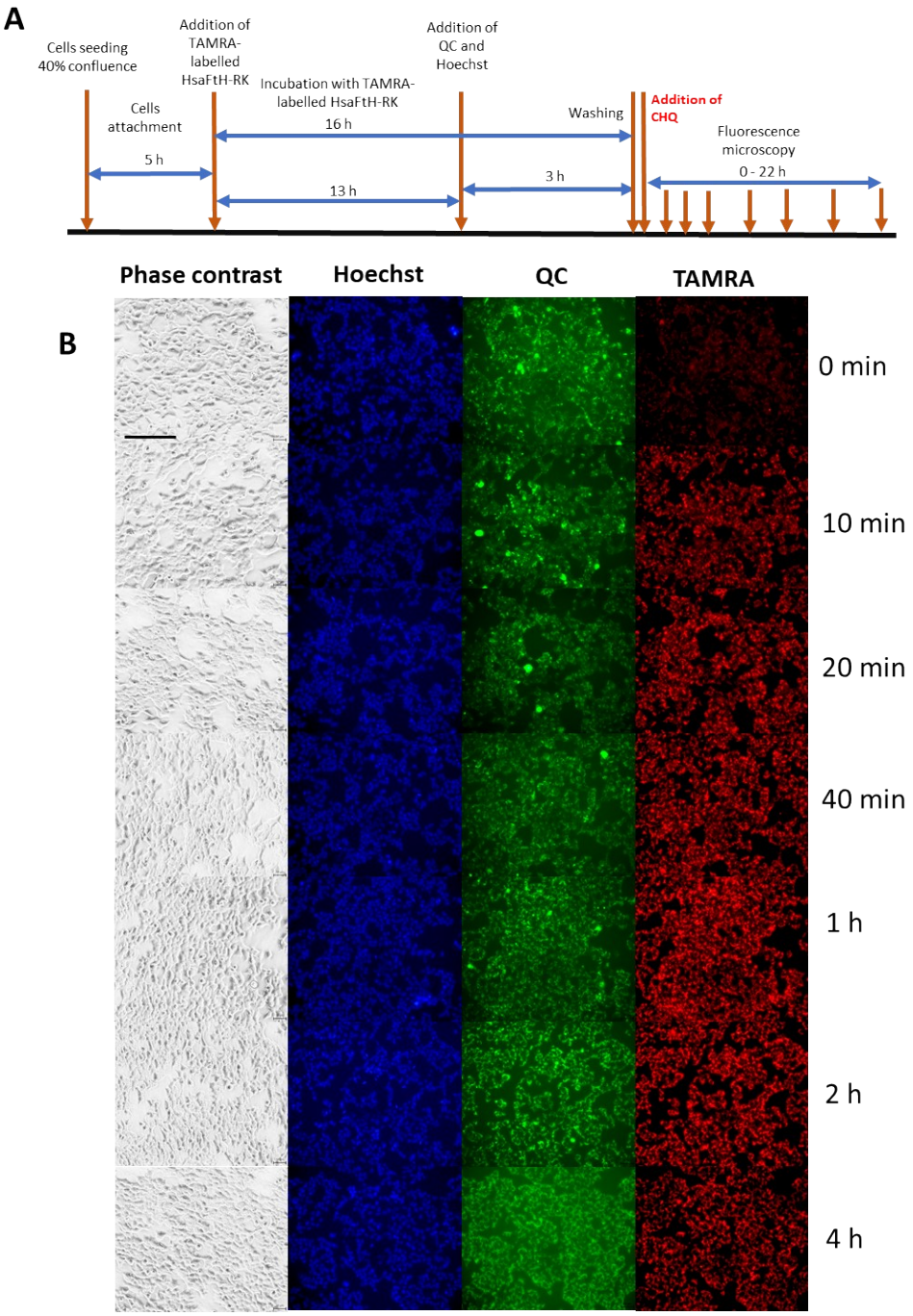

Fig. S12: HEK-293 cells treated with TAMRA-HsaFtH-RK. The acidic endolysosomal compartments are stained using QC. The cells were treated with 100 µM CHQ in order to disrupt endolysosomal compartments. (**A**) Schematic drawing of experiment time-course and treatment regimes. (**B**) Phase contrast and fluorescence micrographs of TAMRA-HsaFtH-RK treated HEK-293 cells in indicated time points. After addition of CHQ a visible increase in TAMRA fluorescence is seen due to de-acidification of the endolysosomes. Nuclei were counterstained using Hoechst 33342. Scale bar, 200 µm.

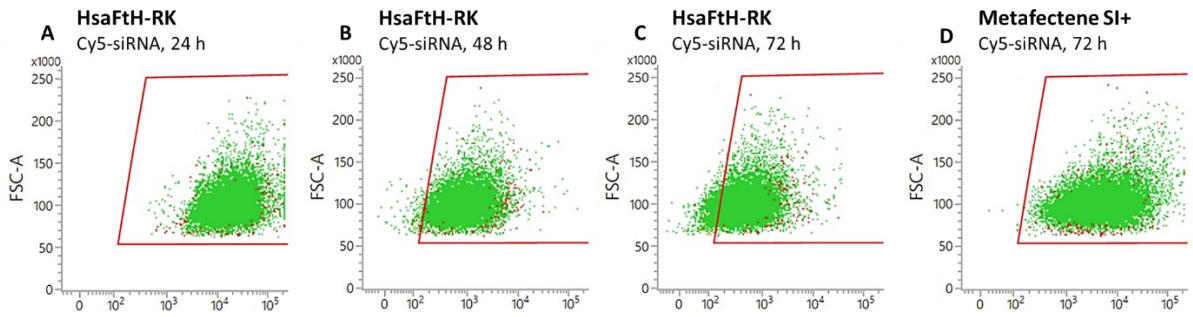

Fig. S13: FACS plots showing the cellular retention of Cy5-siRNA transfected by HsaFtH-RK (**A**, **B**, **C**), and Metafecten SI+ (**D**) after 24 h (**A**), 48 h (**B**) and 72 h (**C**, **D**). X-axis: The fluorescence of Cy5-siRNA.

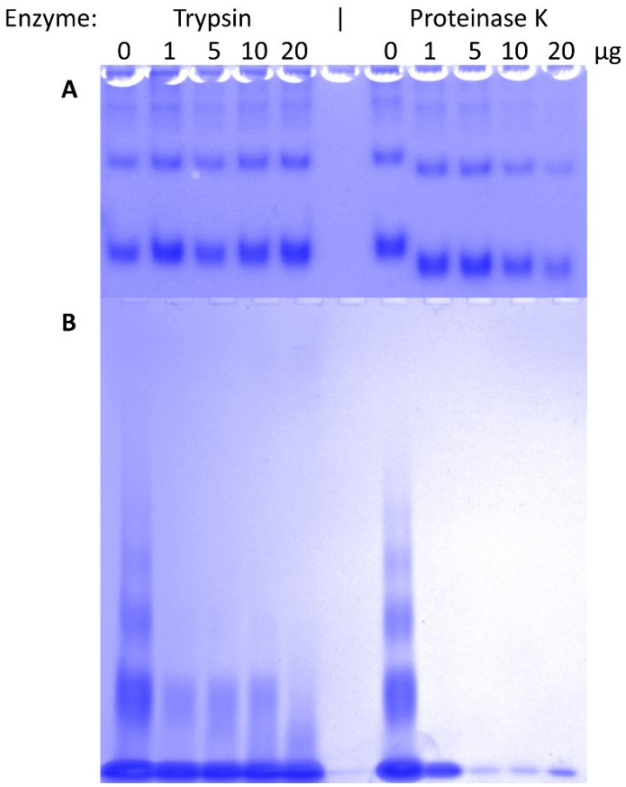

Fig. S14: Proteolytic digestion of (**A**) HsaFtH-RK, and (**B**) BSA by increasing amounts of proteolytic enzymes (incubated for 1 h at 37°C) under native conditions separated in native PAGE stained by CBB.

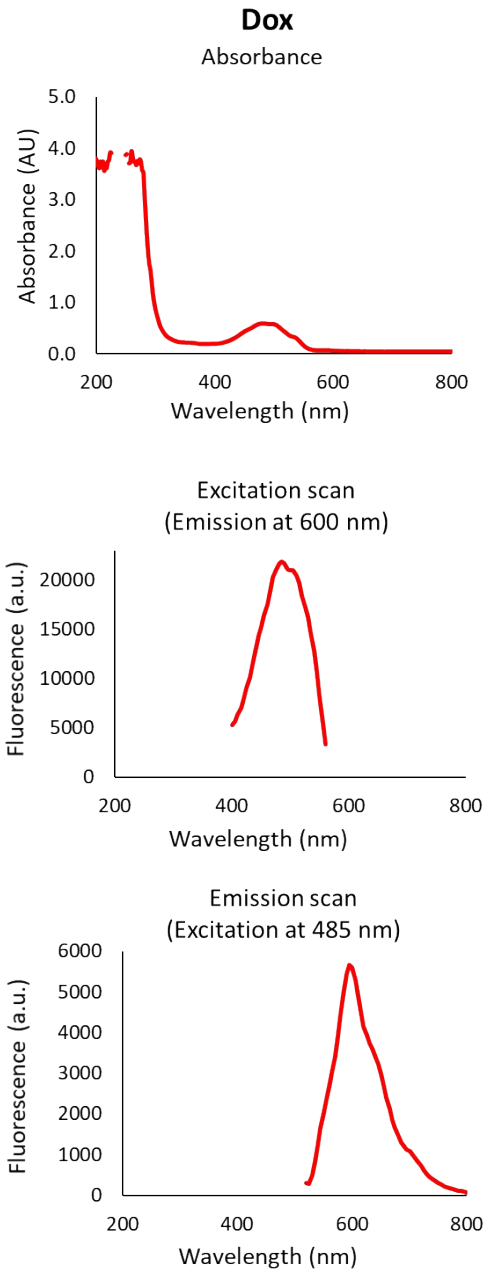

Fig. S15. Absorption and fluorescence spectra of 50 μM Dox dissolved in DMSO.

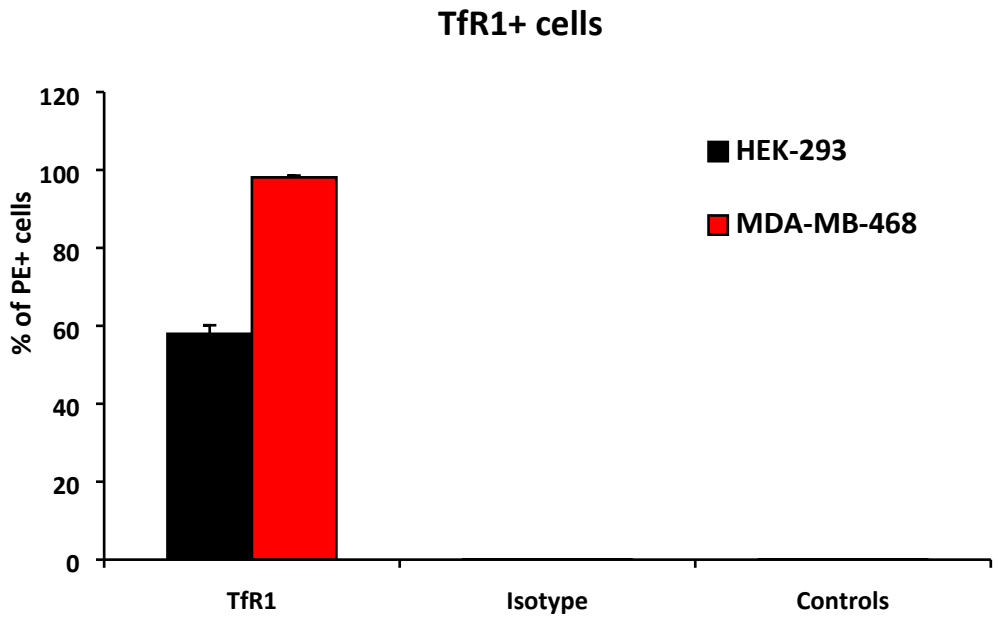

Fig. S16: The expression of ferritin receptor TfR1 in selected cell lines.